Pure & Appl. Chem., Vol. 57, No. 8, pp. 1071–1082, 1985.
Printed in Great Britain.

Data on transport properties of electrolyte solutions for applied research and technology

J. Barthel and H.-J. Gores

Institut für Physikalische und Theoretische Chemie der Universität Regensburg, Fed. Rep. Germany

Abstract - Transport properties, conductance of electrolyte solutions and viscosity of their solvents, as well as dielectric properties are discussed in the framework of applications in modern technology. Electrolyte solutions in high energy batteries with lithium anodes are chosen for exemplifying both the role of the solvent and the fulfilment of supplementary conditions imposed by technical applications. The generation of electrolyte property profiles by means of a data base is used and the data and method base for electrolyte solutions, ELDAR, is presented.

INTRODUCTION

A perusal of recent literature shows the increasing importance of ion-conducting materials in various fields of applied research and technology (refs. 1-3, and quoted literature). Solid ion conductors (crystallines, composites, and glasses), salt melts and electrolyte solutions are all materials exhibiting inherently useful properties. In comparison with solid ion conductors, electrolyte solutions provide better levelling properties, both for temperature and concentration gradients, permanent contact between electrodes and the ionic conductors,and generally higher conductivities at ambient temperatures (Table 1). Leakage and corrosion problems and lower transference numbers of the active ions are drawbacks. Nonaqueous, as compared to aqueous electrolyte solutions, exhibit larger liquid ranges, wider cathodic and anodic stability ranges (Table 2) and increased solubility for organic materials, but entail higher costs, toxicity, flammability, and generally lower conductivities (Table 1). Recently, low temperature melts offering high conductivities have become available (ref. 20) and these might compete with electrolyte solutions when some technological problems are solved.

There are numerous examples of actual applied research where nonaqueous electrolyte solutions have yielded convincing, and in many cases, unique results: primary and secondary batteries of high energy density and good low-temperature performance, electroplating of aluminum and refractory metals, electrodeposition of various materials and related processes, flat non-emissive electrode displays, photoelectrochemical cells, wet capacitors, and various fields of electro-organic synthesis (refs. 1-3).

In this paper some features of the transport properties of electrolyte solutions are discussed which might be helpful for applied research.

PROCUREMENT OF ELECTROLYTE DATA

A most important obstacle to systematic research of nonaqueous electrolyte solutions in technology is the lack of comprehensive information and engineering data. Procurement of electrolyte data is often a difficult and time-consuming procedure. Data are widely spread in the literature; many results which were obtained by resolving special problems could be useful for others in quite different fields of application. Up to now there exist neither comprehensive tables of reliable electrolyte data nor a general treatment of this class of solutions, especially for the most important mixed-solvent systems. This situation stimulated the development of the ELDAR (Electrolyte Data Regensburg) data base (refs. 5-7), Fig. 1.

Actually ELDAR provides about 8,000 references, 180,000 data tuples and 15,000 key words in a thesaurus of polyhierarchical structure. The data of ELDAR are available via the DECHEMA data bank DETHERM. Methods and equations of ELDAR permit the generation of property profiles, i.e. tables or plots of electrolyte properties as a function of electrolyte concentration, solvent composition, temperature or pressure, which are helpful for the lay-out of technical problems. Examples are given in the following text. Data basis vectors and rules for "best" values simplify this procedure.

TABLE 1. Comparison of specific conductances (κ) and activation energies of tranport (E_a) for various ion conductors.

Type	material and conducting ion		Temp/°C	10^3 κ/Scm^{-1}	E_a/kJ mol^{-1}	Ref.
SOLIDS crystalline	Li_3N	Li^+	25	0.2 to 1	9.6;28	8,9
	$Li_{14}ZnGe_4O_{16}$(LISICON)	Li^+	300	0.5 to 10	18,3	8,62
	$Na_2O \cdot n\ Al_2O_3$(β-alumina)	Na^+	25	1	15.4 ± 1.0	10
	$RbAg_4I_5$	Ag^+	25	250	6.7	10
	$H_3PMo_{12}O_{40} \cdot 29\ H_2O$	H^+	25	180	-	11
composite	LiI/Al_2O_3	Li^+	25	10^{-3} to 0.1	42.5	8
	$LiC_2O_2F_3/(PEO)_{4.5}$	Li^+	25	10^{-5}	-	12
	$LiClO_4$/polyvinylidene fluoride	Li^+	25	10^{-3}	>72	13
	$LiCF_3SO_3/(PEO)_{8.1}$	Li^+	~50	10^{-3}	107 ± 13	14
	PEO = polyethylene oxide					
glass	$LiI/Li_2S/P_2S_5$(45/37/18)	Li^+	25	10^{-2} to 1.3	>30;38	15-17
	GeS_2/Li_2S(50/50)	Li^+	25	4×10^{-2}	49	15,62
	$Ag_7I_4AsO_4$	Ag^+	25	10	-	10
MELTS	LiCl		637	5854	-	18
	KCl		797	2229	-	18
	LiCl/KCl (eutectic melt)		457	1615	-	18
	$LiClO_3$		131.8	115	-	19
	Ethylpyridinium bromide/$AlCl_3$ (1:2)		25	8.43 to 16.9	-	20
SOLUTIONS aqueous	4.8 M H_2SO_4/H_2O (lead acid battery, charged)		20	700	-	21
	0.8 M H_2SO_4/H_2O (lead acid battery, discharged)		20	300	-	21
	KOH/H_2O (6.93 mol kg^{-1})		20	620	-	22
	2.81 M $LiClO_4/H_2O$		25	151.7	-	23
nonaqueous	$LiClO_4$/PC (0.66 mol kg^{-1})		25	5.42	16.2(15°C)	24
	$LiClO_4$/PC,DME(42 w/o PC)(1.39 mol kg^{-1})		25	14.6	10.7(15°C)	25
	$LiAsF_6$/PC,DME(32 w/o PC)(1.13 mol kg^{-1})		25	17.4	-	26
	$LiClO_4$/Methanol (3.92 mol kg^{-1})		25	49.8	10.6(15°C)	27
	PC = propylene carbonate, DME = 1.2 dimethoxyethane					

TABLE 2. Stability ranges (voltage windows) of various technically used ion conductors

Type	material	voltage window in Volts	Ref.
SOLIDS crystals	Li_3N	0 to 0.44 vs. Li/Li^+	11
	due to kinetic hindrance	to ⩾ 2 at $i < 1$ mA cm^{-2}	8
	$LiAlCl_4$	1.68 to 4.36 vs. Li/Li^+	11
composite	LiI/polyethylene oxide	-2.1 to 0.7 vs. Ag/Ag^+	8
MELTS	$LiNO_3/KNO_3$(135°C)	2.5 to 4.2 vs. Li/Li^+	28
	Butylpyridinium chloride/$AlCl_3$	-0.4 to 2.0 vs. Al/Al^{3+}	4
	$LiClO_3$	3.2 to 4.6 vs. Li/Li^+	19
SOLUTIONS aqueous	HCl/H_2O	-0.3 to 1.1 vs. SCE	29
	$NaOH/H_2O$	-0.91 to 0.72 vs. SCE	29
nonaqueous	$NaClO_4$/Acetonitrile	-3.5 to 2.4 vs. $Ag/AgClO_4$	30
	$NaBF_4$/Acetonitrile	to +4 vs. $Ag/AgClO_4$	30
	$Bu_4N\ PF_6$/Propionitrile	-2.6 to 3.5 vs. Ag/AgCl	31
	$LiAsF_6$/2-Methyltetrahydrofuran	to +4.32 vs. Li/Li^+ at 1 mA cm^{-2}	32
	$LiAsF_6$/Dioxolane	to +3.6 vs. Li/Li^+ at 1 mA cm^{-2}	32

It is satisfactory to state that modern electrolyte theory is helpful for optimizing forth - coming technologies. On the other hand, exciting new problems arise from technological investigations which then stimulate the theory to search for new approaches.

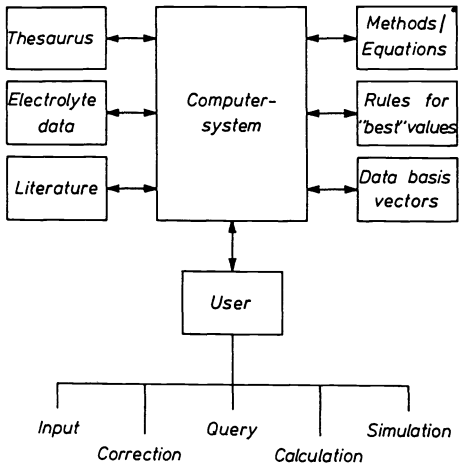

Fig. 1. The ELDAR data base concept (refs. 5-7)

METHODS AND EQUATIONS OF ELDAR

Methods and equations for calculating the properties of electrolyte solutions from infinite dilution to saturation depend on the concentration range investigated. Today Hamiltonian models on the McMillan-Mayer-Friedman (MMF) level are almost exclusively used at low to moderate electrolyte concentrations ($c < 1$ mol dm^{-3})(refs. 33,34). The treatment of concentrated solutions either uses the model of cooperatively rearranging domains (CRD) or rationalizes the effects due to ion-ion and ion-solvent interactions in terms of the parameters characterizing the behaviour of electrolytes in dilute and moderately concentrated solutions (refs. 1,2). Multicomponent systems are generally subjected to data analysis based on purely empirical equations for fitting, interpolation and optimization of property parameters.

HAMILTONIAN MODELS

MMF-level Hamiltonian models use pairwise additive potential functions of the solvent-averaged forces between the ions for calculations of the solution properties; the mean spherical approach (MSA), the Percus-Yevick (PY) equation, and the hypernetted chain (HNC) approximation being the methods used for moderately concentrated solutions. Figure 2 shows the pair correlation functions $g_{+-}(r)$, $g_{++}(r)$ and $g_{--}(r)$ for methanol solutions of potassium iodide at two molalities, 0.05 and 0.5 mol kg^{-1}, calculated from vapour pressure measurements (refs. 34,35). Calculation is based on Friedman's HNC soft sphere model (ref. 77).

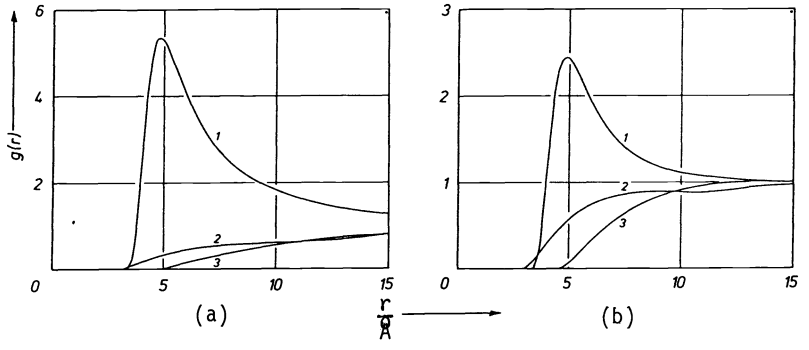

Fig. 2. Pair correlation functions $g_{+-}(1)$, $g_{++}(2)$, $g_{--}(3)$ for methanol solutions of KI at 0.05 m (a) and 0.5 m (b)

Pair correlation functions $g_{ij}(r)$ are related to their potentials of mean force by the help of relationships

$$g_{ij}(r) = \exp\,[-W_{ij}(r)/kT] \qquad (1)$$

Extrapolation of the pair correlation functions of equally charged ions to low concentrations shows that the population of equally charged ions at short mutual distances (about one or two solvent molecules) can be neglected at low concentrations.

Low concentrations are the domain of application of the chemical model (CM) of electrolyte solutions (refs. 1,2,5,36,37) which subdivides the space around an ion into three regions:

(i) $r < a$, a being the minimum distance of two ions, i and j, which is assumed to be the sum of the effective ion radii,
(ii) $a \leqslant r \leqslant R$, the region of short-range interactions which can be occupied only by paired states of oppositely charged ions,
(iii) $r \geqslant R$, the region of long-range interactions.

Region (i) is characterized by a hard-sphere potential. The mean-force potentials of regions (ii) and (iii) are split into two parts representing the coulombic, W_{ij}^{el}, and noncoulombic, W_{ij}^{*}, interactions.

$$W_{ij}^{(\beta)} = W_{ij}^{el(\beta)} + W_{ij}^{*(\beta)}; \quad \beta = \text{(ii) or (iii)} \tag{2}$$

The ion-pair association concept for symmetrical electrolytes can easily be introduced into the chemical model, by assuming that the distance parameter R equals the upper limit of ion association. Then the association constant at concentration c is given by the relationship

$$\frac{1-\alpha}{\alpha^2 c} = K_c = 4000\,\pi\,N_A \int_a^R r^2\, g_{+-}^{(ii)}\, dr \tag{3}$$

Properties of electrolyte solutions, E(c;p,T), from low to moderate concentrations can be represented by a set of equations (refs. 1,5)

$$E(c;p,T) = E^{\infty}(p,T) + E'(\alpha c;p,T;R,W_{+-}^{*}); \quad \frac{1-\alpha}{\alpha^2 c} = K_c \tag{4a,b}$$

where $E^{\infty}(p,T)$ is the corresponding property of the infinitely dilute solution, K_c is the concentration-dependent constant according to Eq. (3) and α is the "degree of dissociation" of the ion pairs. The chemical potential μ_Y of an electrolyte compound, $Y = C_{\nu_+}^{z_+} A_{\nu_-}^{z_-}$,

$$\mu_Y(c;p,T) = \mu_Y^{\infty}(p,T) + \nu RT \ln \alpha c_{\pm} y_{\pm}' \tag{5}$$

and hence all thermodynamic properties based on Eq. (5), such as the equations of solution and dilution processes (ref. 1), as well as the transport equations, e.g. conductance equations

$$\Lambda(c;p,T) = \Lambda^{\infty}(p,T) - \Lambda^{el}(\alpha c;p,T;R,W_{+-}^{*}) - \Lambda^{rel}(\alpha c;p,T;R,W_{+-}^{*}) \tag{6}$$

or kinetic and spectroscopic equations, are equations of the type given by Eq. (4a).

The chemical model allows the determination of values R and W_{+-}^{*}, which are independent of the particular thermodynamic or transport property being investigated, as well as reliable values of $E^{\infty}(p,T)$, by well-founded extrapolation methods. This feature is used in ELDAR for the simulation of solution properties. As an example, Fig. 3 shows the plot of completely calculated conductance functions without the use of conductance data (ref. 38). The results of independent conductance measurements (o and ◇) are added to prove the validity of the method.

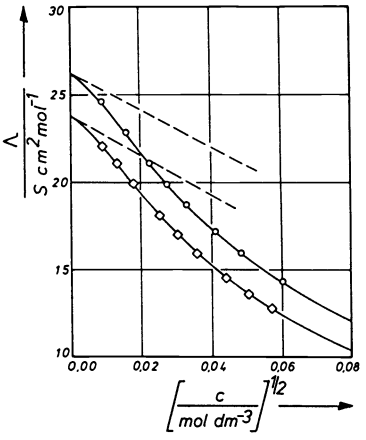

Fig. 3. Conductance of propanol solutions of Pr_4NI(o) and i-Am_4NI (◇) at 25°C

The full lines are calculated with the help of an equation of the type given by Eq. (6) using R and W_{+-}^{*} values from calorimetric measurements and single ion conductance based on transference numbers $t_{+}^{\infty}(K^+/PrOH)$. The broken lines represent the Onsager limiting law of conductance.

A comprehensive investigation of solution properties in various solvents and with a multitude of electrolytes has yielded an important result: Distance parameters R can be set for all property equations from chemical evidence: R = a + ns, a being the centre-to-centre distance of closest approach of cation and anion in the solvent and s being the dimension of an orientated solvent molecule, n = 0, 1, or 2. Solvents and solutes may be arranged in classes permitting the *a priori* estimation of R (refs. 1,2,5,38).

Integral equation methods, MSA, PY, and HNC, have not so far been used to a significant extent for providing data for technology. A conductance equation on the HNC level was recently pub-

lished by Altenberger and Friedman (ref. 39); MSA approaches on conductance are due to Ebeling and Grigo (ref. 40).

For MMF-level Hamiltonian models there is an upper limit to the ion concentration range within which it is sensible to compare the model with data for real systems if the pairwise-addition approximation is made (ref. 33). This limit depends on the nature of solute and solvent and may occur at very low concentrations in certain cases; e.g., for lithium salts in electron donor solvents of low permittivity such as dimethoxyethane triple-ion formation and a change in the sign of the temperature coefficient of molar conductance indicate that this limit is surpassed at concentrations of about 10^{-4} mol dm^{-3} (ref. 41).

THE CONCEPT OF COOPERATIVELY REARRANGING DOMAINS

Practising engineers use Pitzer's equation (ref. 42) or similar equations (ref. 43) for the reduction of thermodynamic data and prediction of the properties of complicated aqueous electrolyte mixtures at high electrolyte concentrations. Transport equations for highly concentrated solutions are not available. However, some help for rationalizing data can be expected from the use of molten salt approaches such as the concept of cooperatively rearranging domains (CRD) as developed by Adam and Gibbs (ref. 44), and Angell et al. (refs. 46-48). We have succeeded in transferring their concept to concentrated nonaqueous solutions (ref. 49); examples are given in the following section. However, success is actually limited to conductivity of electrolyte solutions showing no or only slight ion-ion association.

The Vogel-Fulcher-Tamann (VFT) equation, based on the CRD concept, can be used in the form

$$F(T) = A(T) \exp [-B/R(T-T^o)] \tag{7}$$

for analyzing the temperature dependence of various transport properties F(T) and for determining the ideal glass transition temperature T^o by appropriate extrapolation methods. The glass transition temperature T^o is considered to be the appropriate reference temperature for all transport and relaxation processes in the solution, F(T) equals zero at T^o. From a thermodynamic point of view, T^o is defined by the postulate of vanishing configurational entropy (ref. 44); another definition uses vanishing free volume V_f to define T^o (ref. 45). The pre-exponential factor, A(T) in Eq. (7), can be used in various forms, but is generally written $A'T^n$, $A(T) = A'T^n$, where n = +1/2, -1/2, 1, or is used as an adjustable parameter (refs. 50, 51). Angell (ref. 52) and Spiro and King (ref. 50) stress that the temperature dependence of A(T) is of minor importance and can even be omitted if $T/T^o < 2$ or if F(T) is any property other than diffusion. We follow their recommendation by setting n = 0. In binary electrolyte solutions at molality m of the solute, the glass transition temperature is assumed to be (ref. 49)

$$T^o(m) = T^o(0) + am + bm^2 \tag{8}$$

In Eq. (8), $T^o(0)$ is the glass transition temperature of the infinitely dilute solution and a and b are adjustable parameters. A comprehensive study on the conductance of PC solutions of 14 electrolytes (ref. 49) shows that $T^o(0)$ for all of them is found equal to the glass transition temperature of pure PC as determined from viscosity measurements. Furthermore, the activation energies of conductance at infinite dilution, $B(0)T^2/(T-T^o)^2$, are equal for all electrolytes and equal to that of viscosity (ref. 49). No difference is found between the activation energies determined by the use of Eq. (7) and those obtained from the application of MMF models (ref. 53).

ELECTROLYTE SOLUTIONS IN HIGH ENERGY BATTERIES

Batteries can be divided into two classes, the non-rechargeable primary and the rechargeable secondary batteries. Actually lithium is the most favoured anode material for ambient temperature high-energy batteries, but other high electrode potential, low equivalent weight elements such as Na, K, Be, Mg, Ca, and Al are studied as potential substitutes. The non-aqueous primary lithium battery is now a fact and is produced in various types and configurations, see Table 3.

In contrast, secondary lithium batteries are not yet commercially available with a single exception of the Exxon Li/TiS_2 episode. However, appreciable success has been made with suitable cathode materials, mainly in the field of the intercalation type (refs. 1,3,59) and doped, conducting polymers (ref. 63). The inherent reactivity of lithium with electrolyte solutions may be reduced by procedures such as those proposed and compiled by Brummer and coworkers (ref. 64). Some results are compiled in Table 4 on lithium cyclability.

TABLE 3. Commercially available primary lithium cells (refs. 1,54-62).

Cathode material	Ion conductor	Volts V	Theor. energy Wh/kg	Theor. energy Wh/dm^3	Pract. energy Wh/kg	Pract. energy Wh/dm^3	Manufacturers
MnO_2	$LiClO_4$;PC/DME	3.5	1000	3097	200	400	Sanyo, VARTA, GE, Duracell, UCC, SAFT, Renata, Toshiba, Hitachi, Matsushita, Berec, Roy-O-VAC, Polaroid
$(CF_x)_n$ $n \sim 1$	$LiAsF_6$;DMSI $LiBF_4$;γ-BL/THF PC/DIOX	2.8 to 3.3	>1992	>2653	200	400	Matsushita, ESB, Panosonic, Eagle-Picher
	DIOX = Dioxolane, DMSI = Dimethylsulfite						
Ag_2CrO_4	$LiClO_4$;PC	3.31	513	2088	275	700	SAFT
V_2O_5	$LiAsF_6$ or $LiBF_4$/MF	3.50	497	1397	200	600	Honeywell
CrO_x	$LiClO_4$;PC/DME	3.7	-	-	270	675	VARTA
CuO	$LiClO_4$;DIOX; DME/DIOX; THF/DME	2.24	1285	3140	275	650	SAFT, Sanyo, Matsushita, Cordis, Ray-O-VAC
FeS_2	$LiClO_4$;PC/DME	1.75	1273	2474	130	385	UCC, Sanyo, Berec
Bi_2O_3	$LiClO_4$;PC/DME	2.04	646	2478	90	350	VARTA
$Bi_2P_2O_5$	$LiClO_4$;DIOX	2.00	546	2318	150	400	SAFT
$SOCl_2$	$LiAlCl_4$; $SOCl_2$/cosolv.	3.66	1477	2005	300-480	650-950	GTE, Tadiran, Honeywell, SAFT, Greatbach
SO_2	LiBr/AN	2.91	1098	1353	280	440	Duracell, Power Conversion, Honeywell, Silberkraft, SAFT
SO_2Cl_2	$LiAlCl_4$; SO_2Cl_2/cosolv	3.9	-	-	500	1000	Greatbach, GTE
PbI_2,PbS	LiI/Al_2O_3(s)	1.87	211	997	75-150	300-600	Catalyst Research,Wilson Greatbach
I_2(P2VP)	LiI(s)	2.8	556	1920	120-200	350-700	Duracell
Me_4NI_5	LiI/SiO_2(s)	2.75	-	-	125	400	-
	P2VP = poly-2-vinylpyridine						

TABLE 4. Efficiency of Li-cycling in various solutions

Electrolyte solutions		Cycling efficiency		Ref.
Solute	Solvent	at 1 C/cm^2	at 25 C/cm^2	
$LiClO_4$	PC	40 %	-	64
	PC + $PSBr_3$	84.5 %	-	64
$LiAsF_6$	DEE/THF (10 $^w/_o$ THF)	> 98 %	96.3 %	65,70
	2-Me-THF	35 cycles at 79 %	-	66
	2-Me-THF + + 2 $^w/_o$ methoxyethanol	900 cycles at 85 %	-	66
	DME	~97 %	90 ± 2 %	67,70
	2-Me-THF	~98 %; 97.5 %	97.5 %	68,69
	tetrahydrofuran (THF)	88 %	58 %	69,70
	diethylether (DEE)	97.9 %	88.9 %	69,70
	DME	97.9 %	-	71
	furan	98 %	-	71
	2-methyl pyrrole	98.2 %	-	71
	3,5 dimethyl isoxazole	98.0 %	-	71

Generally, the requirements for lithium battery electrolyte solutions are
- high specific conductance to reduce internal resistance
- high solubility of the electrolyte to reach appropriate electrolyte concentrations
- low solubility of the cathode material
- chemical and electrochemical stability and compatibility with electrode materials
- high mobility of the active ion (Li^+) to reduce concentration polarization.

The compatibility conditions are hard to fulfil. It is now generally accepted that no solvent is thermodynamically stable with lithium; only kinetic stability can be obtained, mainly due to the formation of conducting solid electrolyte interfaces (SEI) on the lithium anode by

reaction of the anode material with the electrolyte solution. In nonaqueous lithium salt solutions SEIs on the lithium anode are observed of about 2 to 10 nm in thickness and of 10^7 to 10^8 Ωcm of resistivity. Typical SEI compositions are Li_2CO_3 (PC solutions of $LiClO_4$), Li_2O or reduction products (2-Me-THF solutions of LiI), or LiCl ($SOCl_2$ solutions of $LiAlCl_4$ or $LiB_{12}Cl_{12}$) (refs. 72,73).

The requirements imposed by the compatibility conditions limit the choice of solvents for battery electrolyte solutions to four main classes
- aprotic protophilic solvents, e.g. DMF, DMSO
- aprotic protophobic solvents, e.g. PC, γ-BL
- low permittivity electron donor solvents, e.g. DMF, THF
- inert solvents, e.g. hydrocarbons.

Among these solvents the most suitable materials for battery application should combine high permittivity, low viscosity and wide liquid range. Aprotic solvents show high permittivities, but also high viscosities and unfortunately strong temperature dependence of viscosity, e.g. Fig. 4 (ref. 1). Ethers and some inert solvents exhibit the opposite behaviour, i.e. low permittivities and viscosities and low temperature coefficients of viscosity. Only mixtures of solvents of different classes, e.g. ethers and dipolar aprotic solvents, show suitable properties by balancing the specific advantages and drawbacks of the pure solvents.

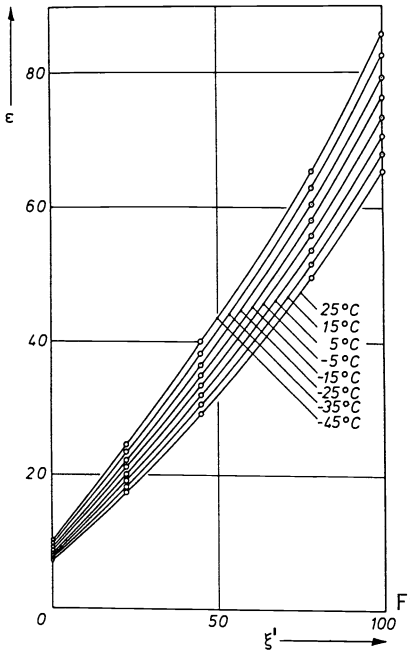

Fig. 4 a

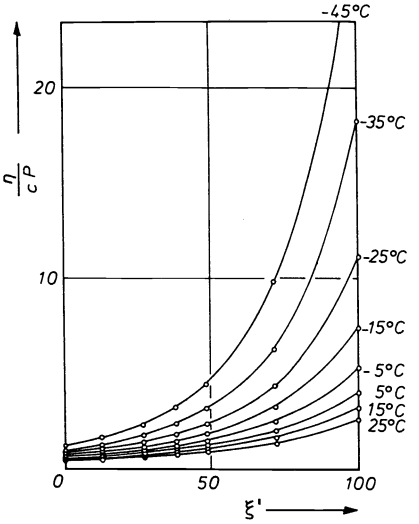

Fig. 4 b

Fig. 4. Relative permittivities (a) and viscosities (b) of PC-DME mixtures ($\xi' = {}^{w}/_{o}$ of PC) at various temperatures

It is sufficient to say that the use of mixed solvents, exemplified in this paper for lithium battery electrolyte solutions, is also a general feature in other fields of application. A comprehensive investigation in our laboratory of nonaqueous electrolyte solutions has been carried out to provide data and rules for the choice of appropriate organic solvent systems for actual technologies. Data on PC, DME, γ-BL, THF, DIOX, AN, MeOH, EtOH, PrOH, 2-PrOH, acetone, and their mixtures (also with H_2O) have been already published or are underway.

Specific conductances κ vs. molalities m at various temperatures yield the usual pattern:- curves with maxima, κ_{max}, at concentrations m = μ. Data are very well reproduced by the empirical Casteel-Amis equation (ref. 76)

$$\frac{\kappa}{\kappa_{max}} = \left(\frac{m}{\mu}\right)^a \exp\left[b(m-\mu)^2 - \frac{a}{\mu}(m-\mu)\right] \qquad (9)$$

Data analysis yields the quantities μ and κ_{max} and the two parameters a and b. Hypothetical values of μ and κ_{max} are obtainable by short extrapolations when limited solubilities prevent the attainment of concentration μ. The possibility of extrapolation and the small number of measurements needed for a complete conductance curve make Eq. (9) more suitable than polynomials in m.

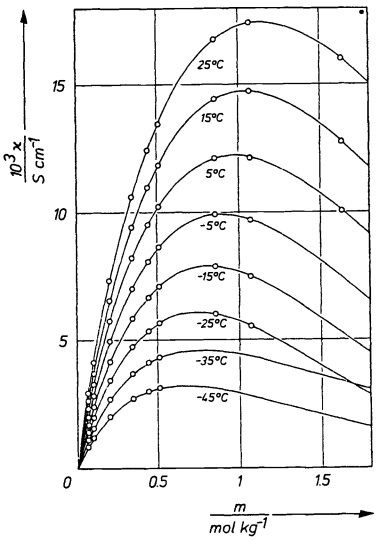

Fig. 5 a. Specific conductances of $LiAsF_6$ solutions in a PC-DME mixture, 32 $^{w}/_{o}$ of PC

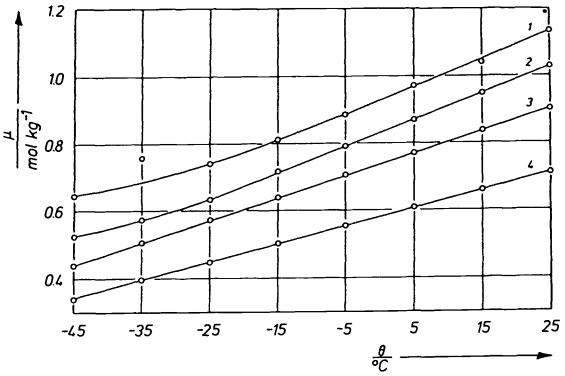

Fig. 5 b. Positions μ of the conductance maxima of $LiAsF_6$ solutions in PC-DME mixtures (ξ = weight fraction of PC) at various temperatures.
ξ = 0.32(1); 0.59(2); 0.81(3); 1(4)

Fig. 5 a shows a computer plot of $\varkappa = \varkappa(m,T)$ for $LiAsF_6$ in a PC/DME (32 $^{w}/_{o}$ PC) mixture. This example was chosen because it exhibits short extrapolations at -35°C and -45°C and because the $\varkappa_{max}$ value of 16.5 mS cm^{-1} at 25°C is among the highest values found for Li-battery electrolytes. Diagrams of this type for various organic solvent systems are now available. The complete information on the maximum conductance of $LiAsF_6$ solutions as a function of the composition of the PC/DME solvent system is given in Figs. 5 b and 5 c. Information on the $LiBF_4$/PC-DME system is added for comparison (Fig. 6).

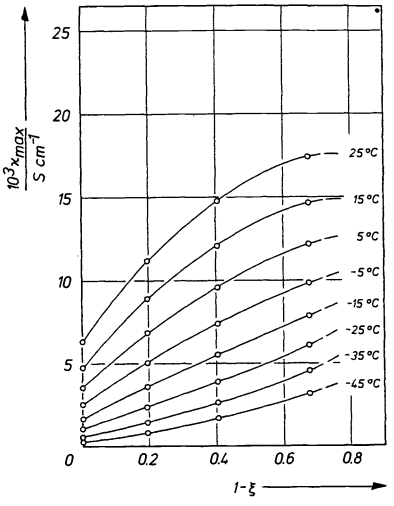

Fig. 5 c. Conductance maxima ($\varkappa_{max}$) of $LiAsF_6$ solutions in PC-DME mixtures at various temperatures (ξ = weight fraction of PC)

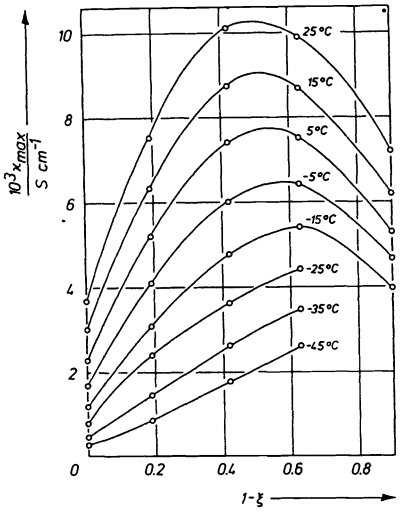

Fig. 6. Conductance maxima ($\varkappa_{max}$) of $LiBF_4$ solutions in PC-DME mixtures at various temperatures (ξ = weight fraction of PC)

Some features of specific conductance may be used for planning electrolyte solutions on the drawing board by the engineer.

The maximum of specific conductance is a general feature of concentrated solutions; it is the consequence of competing effects, increasing charge density and decreasing ion mobility with increasing electrolyte concentration (ref. 25); it is observable, however, only at sufficiently large solubility. The position of the maximum at concentration μ depends on the structure of the electrolyte solution. A rough estimate based on the assumption of cubic dense packing of the ions in the solution shows that the mean ionic distances at concentration μ are of the

order of magnitude of one to two solvent molecules in PC (aprotic solvent) and of the length of an OH-group in MeOH (protic solvent) solutions of 1,1 electrolytes.

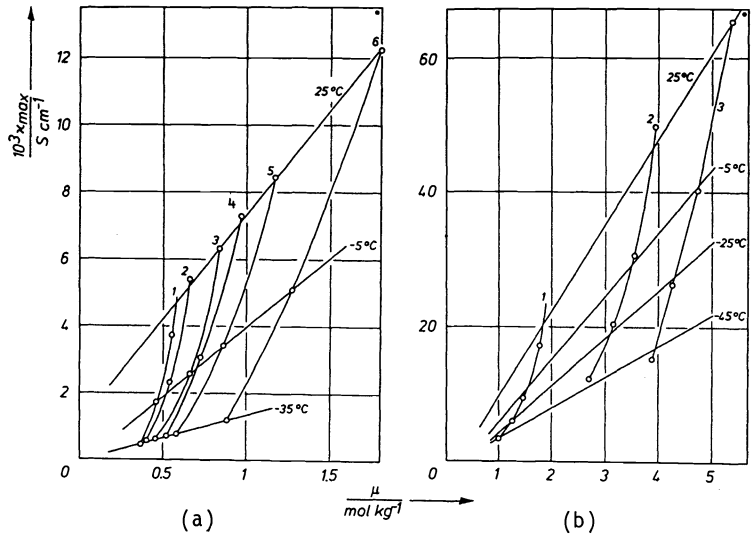

Fig. 7. Linear correlations κ_{max} vs. μ at various temperatures
(a): PC solutions of $LiBF_4$(1); $LiClO_4$(2); Bu_4NPF_6(3); KPF_6(4); Pr_4NPF_6(5); Et_4NPF_6(6)
(b): MeOH solutions of Bu_4NBr(1); $LiClO_4$(2); Me_4NCl(3)

Plots of κ_{max} vs. μ are approximately linear; high concentrations μ entail high maximum values of specific conductance κ_{max}. Figure 7 shows this linear correlation for PC and MeOH solutions at various temperatures. For the sake of clearness only few electrolytes are exhibited, for the full information on a large number of electrolytes at 25°C see refs. 24,27,53. Electrolyte solutions in methanol show two classes of solutes, large tetraalkylammonium salts with small μ values and alkali metal salts with large μ values in agreement with the short-range (non coulombic) interaction potentials calculated from dilute solutions. The sequence in PC solutions rather depends on the ionic Stokes' radii. Permittivity measurements on MeOH and PC solutions reflect the same classification (ref. 53).

Temperature dependence of specific conductance is appropriately reproduced by a family of $\kappa_m(T)$ functions (specific conductances at constant molality as a function of temperature) with the help of VFT equation, Eq. (7).

$$\kappa_m(T) = A_m^{(\kappa)} \exp\left[-\frac{B_m^{(\kappa)}}{R(T-T^0(m))}\right] \qquad (10)$$

The functions $T^0(m)$ and $B_m^{(\kappa)}$ are characteristic of the solute in a given solvent, yielding, however, equal limiting values $T^0(0)$ and $B_0^{(\kappa)}$ for all of them (ref. 49). Activation energies of transport process $E_a^{(\kappa)}(m,T)$, $E_a^{(\kappa)} = -R[d \ln \kappa_m/d(1/T)]$, of all solutes are equal at concentrations zero and μ, $m = 0$ and $m = \mu$, respectively. This observation may be rationalized by the assumption of a characteristic energy barrier of the solvent, mainly depending on its viscosity, which is overcome at concentration μ. Very high values of μ are observed for ether solutions entailing high specific conductances which otherwise can hardly be understood; 1,1 electrolytes in ether solutions exhibit association constants of 10^6 mol^{-1} dm^3 and more.

If association is negligible, e.g. in PC solutions, conductivity is determined up to rather high concentrations by the cation radii (R_4N^+ salts) or by the Stokes radii (alkali metal salts), e.g. for R_4NPF_6, linear functions of (κ/m) vs. r^{-1} are observed up to 1 molal solutions, Fig. 8.

Decreasing viscosity, both by increase of temperature and addition of cosolvent, increases ion mobilities. This effect is opposed by the less significant decrease in permittivity which diminishes the number of charge carriers and by changes in solvation when solvent mixtures are used. DME molecules are apt to act as a bidentate ligand for Li^+ ions with molecular dimensions of the Li^+ solvating 12-crown-4 ether thus entailing a significant change in the mobility function (κ/m) for DME-poor mixtures of the PC/DME solvent system (ref. 25); $\kappa_{max}(\xi)$ functions of lithium salts in these solutions show a larger increase when compared to those of other alkali metal salts; specific solvation of Li^+ ions by DME has also been proved independently by other methods (ref. 74).

Viscosity decrease resulting from both increased temperature and cosolvent addition acts in the same direction proving that solvent viscosity is the main property controlling the energy

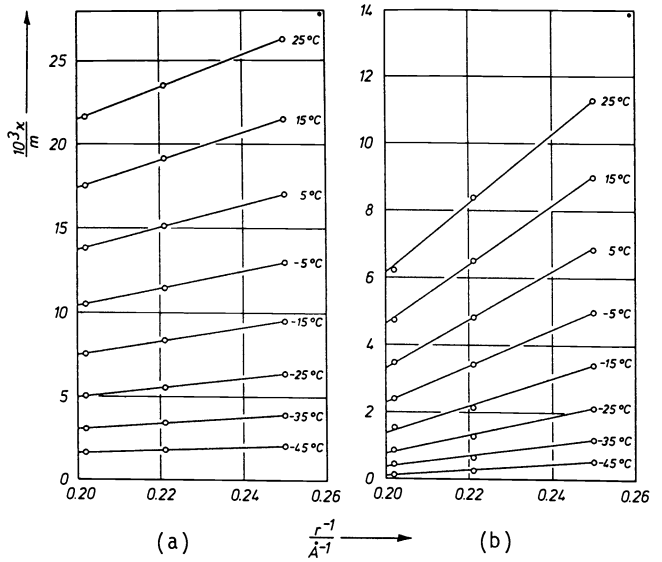

Fig. 8. Mobility functions (κ/m) vs. reciprocal radii of cations R_4N^+ (R = Et, Pr, Bu) in PC solutions of R_4NPF_6 salts at constant salt concentrations, (a) 0.1 m, (b) 1 m

barrier of the transport process. The decrease of solvent viscosity reduces the activation energy E_a of transport, $E_a = f(m)$, and hence causes the shift of μ values to higher concentrations, see Fig. 5 b. The absolute maximum κ^*_{max}, i.e. the maximum of κ_{max} as a function of solvent composition $(1-\xi)$ or temperature Θ, also increases with decreasing viscosity. Decreasing ion-ion association acts in the same direction, e.g. κ^*_{max} increases in the series $LiBF_4$ (Fig. 6) < $LiClO_4$ (ref. 25) < $LiAsF_6$ (Fig. 5 c) and so does the $(1-\xi^*)$ value (solvent composition ξ at which κ^*_{max} is attained). The same permittivity effect causes the shift of $(1-\xi^*)$ for each electrolyte at varying temperature (Figs. 5 c and 6); maxima (κ^*_{max}) are attained at higher $(1-\xi^*)$ values with decreasing temperature (increasing permittivity).

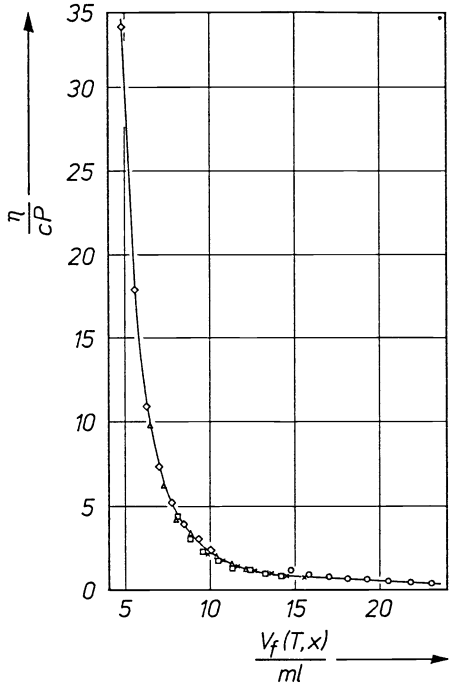

Fig. 9. Viscosity η of PC-DME mixtures (x = mole fraction of PC) as a function of free volume at various temperatures x = 0(o); 0.38(x); 0.48(□); 0.71(Δ); 1(◇)

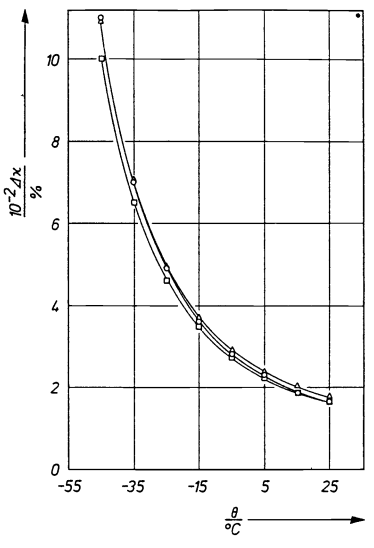

Fig. 10. Relative increase of conductance ($\Delta\kappa/\%$) caused by the addition of DME to PC-solutions (up to 1000 % at -40°C!); (o) $LiClO_4$, ξ = 0.28; (Δ) $LiAsF_6$, ξ = 0.32, (□) $LiBF_4$, ξ = 0.37; ξ = weight fraction of PC; for the definition of $(\Delta\kappa/\%)$ see text.

Important information on transport properties is obtained from the study of viscosity. Unfortunately, such data are lacking in literature, especially for solvent mixtures and temperature dependences.

A comprehensive investigation of viscosity equations for solvent mixtures (ref. 75) led us to favour two-parameter equations of the McAllister type which reproduce viscosities with high reliability and accuracy from a limited number of measurements. Again, FVT equations yield important results. From a series of measurements on PC/DME mixtures at various temperatures, Fig. 4b, ideal glass transition temperatures $T^o(\xi)$ reaching from (49.1 ± 0.7)K for pure DME to (152.2 ± 0.6)K for pure PC can be obtained by nonlinear fitting methods. Based on glass transition temperature, "expansion free volumes, V_f" are obtained with the help of appropriate density functions $\rho(x,T)$ (x = mole fraction of PC)

$$V_f = V(x,T) - V_o(x,T^o) \qquad (11)$$

Figure 9 shows that the viscosity of the mixed solvent system can be represented by a master curve. Deviations of the points are due to errors in extrapolations, the extrapolation ranges (especially for DME) being extended. The positions of measured points on the master curve show that effects on the free volume, excess volume (composition dependence) and thermal expansion (temperature dependence), are theoretically accounted for by this approach which is far better than the usual approaches.

It seems interesting to visualize the success of the mixed-solvent approach on conductivity. Figure 10 shows the relative increase of conductivity $\Delta\kappa(\%)$, $\Delta\kappa(\%) = [(\kappa_{max,mixt} - \kappa_{max,PC})/\kappa_{max,PC}]\cdot 100$; the compositions of the solutions are chosen such that κ_{max} is very close to κ^*_{max}. The reason why all functions are identical within a limit of only 10 % (despite widely varying κ_{max} values), is not yet clear.

REFERENCES

1. J. Barthel, H.-J. Gores, G. Schmeer and R. Wachter, Topics in Current Chemistry, Ed. by F. L. Boschke, Springer, Heidelberg, 111, 33-144 (1983); with 950 references.
2. J. Barthel, H.-J. Gores, G. Schmeer and R. Wachter, Electrolyte Solutions: A Generalized Systematic View, CRC Press, Boca Raton (in preparation).
3. H.-J. Gores and J. Barthel, Naturwissenschaften 70, 495-503 (1983).
4. H. Li Chum and A. R. Osteryoung, Ionic Liquids, Ed. by D. Inman and D. G. Lovering, Plenum Press, New York, 407-423 (1981).
5. J. Barthel, Proceedings of the 9th International CODATA Conference, Ed. by P. Glaeser, North Holland, Amsterdam (in press).
6. C. H. Jacob, A. Scholz, R. Eckermann and M. Klöffler, Entwicklung computergestützter Berechnungsmethoden für Stoffdaten, DECHEMA, Frankfurt/Main 1984.
7. J. Barthel, H. E. Popp and G. Schmeer, Databank ELDAR, BMFT-Projekt NTS 2036; cf. Regensburger Univ.-Z. 10, 14-15 (1985).
8. B. C. Tofield, Ed. Advances Electrochemical Energy Storage Devices, final report, Comm. Eur. Communities [Rep.] Eur 1982, EUR 7595, Vol. 2, Contracts No 315-78-1 EE-DK, 316-78-1-EE-UK, EC SG-EEG-EAEL Oxfordshire, Odense, ECSC-EEG-EAEC, Brussels (1981).
9. U. v. Alpen, J. Solid State Chem. 29, 379-392 (1979).
10. A. R. West, Solid State Chemistry and its Applications, Wiley, New York (1984).
11. R. A. Huggins, Materials for Advanced Batteries, Ed. by D. W. Murphy, J. Broadhead and B. C. H. Steele, Plenum Press, New York 91-110 (1980).
12. W. B. Johnson and W. L. Worrell, Solid State Ionics 5, 367-370 (1981).
13. H. Ohno, H. Matsuda, K. Mizoguchi and E. Tsuchida, Polymer Bull. 7, 271-275 (1982).
14. J. E. Weston and B. C. H. Steele, Solid State Ionics 2, 347-354 (1981).
15. J. L. Souquet, Solid State Ionics 5, 77-82 (1981).
16. J. P. Duchange, J. P. Mulagani and R. Robert, Progr. Batt. & Solar Cells 4, 46-48 (1982).
17. J. P. Malugi, B. Fahys, R. Mercier, R. Robert, J. P. Duchange, S. Baudry, M. Broussely and J. P. Gabano, Solid State Ionics, submitted.
18. G. Mamantov, Materials for Advanced Batteries, Ed. by D. W. Murphy, J. Broadhead and B. C. H. Steele, Plenum Press, New York 111-122 (1980).
19. Sue-Chee S. Wang and D. N. Bennion, J. Electrochem. Soc. 130, 741-747 (1983).
20. R. A. Carpio, L. A. King, R. E. Lindstrom, J. C. Nardi and C. L. Hussey, J. Electrochem. Soc. 126, 1644-1650 (1979).
21. K. J. Euler, Batterien und Brennstoffzellen, Springer, Berlin (1982).
22. Handbook of Batteries and Fuel Cells, Ed. by D. Linden, Tab. C 6, McGraw Hill Book Co, N. Y. (1984).
23. R. Haase and K.-H. Drücker, Z. Phys. Chem. N.F. 46, 140-159 (1965).
24. J. Barthel, H.-J. Gores and G. Schmeer, Ber. Bunsenges. Phys. Chem. 83, 911-920 (1979).
25. H.-J. Gores and J. Barthel, J. Solution Chem. 9, 939-954 (1980).
26. J. Barthel, P. Carlier and H.-J. Gores, Ber. Bunsenges. Phys. Chem. (in preparation).
27. F. Feuerlein, Dissertation, Regensburg 1983.

28. I. D. Raistrick, J. Poris and R. A. Huggins, Proceedings of the Symposium on Lithium Batteries, Ed. by H. V. Venkatasetty, Proc. Vol. 81-4, The Electrochemical Society, Pennington, 477-483 (1981).
29. R. N. Adams, Electrochemistry at Solid Electrodes, Dekker, N. Y. (1969).
30. C. K. Mann, Electroanalytical Chemistry, Vol. 3, Ed. by A. J. Bard, Dekker, New York, 57-134 (1969).
31. J. Heinze, Angew. Chemie 96, 823-840 (1984).
32. H. H. Horowitz, J. I. Habermann, L. P. Kleemann, G. H. Newman, E. L. Stogryn and T. A. Whitney, Proceedings of the Symposium on Lithium Batteries, Ed. by H. V. Venkatasetty, Proc. Vol. 81-4, The Electrochemical Society, Pennington, 131-143 (1981).
33. H. L. Friedman, Faraday Discuss. Chem. Soc. 64, 7-15 (1977).
34. J. Barthel, G. Lauermann and R. Neueder, The Encyclopedia of Physical Science and Technology, Ed. by R. A. Meyers, Academic Press, Inc. (in press).
35. G. Lauermann, Dissertation, Regensburg 1985.
36. J. Barthel, Ber. Bunsenges. Phys. Chem. 83, 252-257 (1979).
37. J. Barthel, Pure Appl. Chem. 51, 2093-2124 (1979).
38. J. Barthel, Phase Equilibria and Fluid Properties in the Chemical Industry, Ed. by European Federation of Chemical Engineering, DECHEMA, Frankfurt a. M. 2, 497-507 (1980).
39. A. R. Altenberger and H. L. Friedman, J. Chem. Phys. 78, II, 4162-4173 (1983).
40. W. Ebeling and M. Grigo, J. Solution Chem. 11, 151-167 (1982).
41. J. Barthel, R. Gerber and H.-J. Gores, Ber. Bunsenges. Phys. Chem. 88, 616-622 (1984).
42. K. S. Pitzer, J. Phys. Chem. 77, 268-277 (1973).
43. J. L. Cruz and H. Renon, AIChE 24, 817-830 (1978).
44. G. Adam and J. H. Gibbs, J. Chem. Phys. 43, 139-146 (1965).
45. M. H. Cohen and D. Turnbull, J. Chem. Phys. 31, 1164-1169 (1959).
46. C. A. Angell, J. Phys. Chem. 70, 2793-2803 (1966).
47. C. A. Angell and R. D. Bressel, J. Phys. Chem. 76, 3244-3253 (1972).
48. C. A. Angell and J. C. Tucker, J. Phys. Chem. 78, 278-281 (1974).
49. J. Barthel, H.-J. Gores, P. Carlier, F. Feuerlein and M. Utz, Ber. Bunsenges. Phys. Chem. 87, 436-443 (1983).
50. M. Spiro and F. King, Ionic Liquids, Ed. by D. Inman and D. G. Lovering, Plenum Press, New York, 57-77 (1981).
51. J. Melsheimer and K. Langner, Ber. Bunsenges. Phys. Chem. 83, 539-544 (1979).
52. C. A. Angell, Aust. J. Chem. 23, 929-937 (1970).
53. J. Barthel, Pure Appl. Chem. 57, 355-367 (1985).
54. J. P. Gabano, Lithium Batteries, Ed. by J. P. Gabano, Academic Press, London 1-11 (1983).
55. H. Ikeda, J. Electrochem. Engineering, Tokyo 179, 40-44 (1981).
56. H. V. Venkatasetty, Lithium Battery Technology, Ed. by H. V. Venkatasetty, Wiley, New York 61-78 (1984).
57. P. Bro and S. C. Levy, Lithium Battery Technology, Ed. by H. V. Venkatasetty, Wiley, New York 79-126 (1984).
58. J. J. Auborn and H. V. Venkatasetty, Lithium Battery Technology, Ed. by H. V. Venkatasetty, Wiley, New York 127-137 (1984).
59. M. Hughes, N. A. Hampson and S. A. G. R. Karunatila, J. Power Sources 12, 83-131 (1984).
60. D. Linden, Handbook of Batteries and Fuel Cells, Ed. by D. Linden, McGraw Hill, New York, Ch. 11 (11-1 to 11-83) (1984).
61. B. B. Owens, P. M. Skarstad and D. F. Untereker, Handbook of Batteries and Fuel Cells, Ed. by D. Linden, McGraw Hill, New York, Ch. 12 (12-1 to 12-24) (1984).
62. K. Shahi, J. B. Wagner and B. B. Owens, Lithium Batteries, Ed. by J. P. Gabano, Academic Press, London 407-448 (1983).
63. J. C. W. Chien, Polyacetylene. Chemistry Physics, and Material Science, Academic Press, Orlando (1984).
64. S. B. Brummer, V. R. Koch and R. D. Rauh, Materials for Advanced Batteries, Ed. by D. W. Murphy, J. Broadhead and B. C. H. Steele, Plenum Press, New York 123-143 (1980).
65. V. R. Koch, J. L. Goldman, J. C. Mattos and M. Mulvaney, J. Electrochem. Soc. 129, 2-4 (1982).
66. P. G. Glugla, J. Electrochem. Soc. 130, 113-114 (1983).
67. J. S. Foos and J. McVeigh, J. Electrochem. Soc. 130, 628-630 (1983).
68. V. R. Koch and J. H. Young, Science 204, 499-501 (1979).
69. S. B. Brummer, Office of Naval Research Contrat Nr. 00014-77-C-0155 Task No. 359-638, Rep. No 10, EiC Laboratories (1982).
70. S. B. Brummer, Lithium Battery Technology, Ed. by H. V. Venkatasetty, Wiley, New York 159-179 (1984).
71. K. M. Abraham and S. B. Brummer, Lithium Batteries, Ed. by J. P. Gabano, Academic Press, London 371-407 (1983).
72. E. Peled, J. Power Sources 9, 253-266 (1983).
73. E. Peled, Lithium Batteries, Ed. by J. P. Gabano, Academic Press, London 43-72 (1983).
74. Y. Matsuda, H. Nakashima, M. Morita and Y. Takasu, J. Electrochem. Soc. 128, 2552-2556 (1981).
75. J. Barthel, H.-J. Gores and M. Utz (in preparation).
76. J. F. Casteel and E. S. Amis, J. Chem. Eng. Data 17, 55-59 (1972).
77. P. S. Ramanathan and H. L. Friedman, J. Chem. Phys. 54, 1086-1099 (1971).